Solar Tower System Temperature Range Optimization for Reduced LCOE

Dr. Reiner Buck[1, a)] and Stefano Giuliano[2, b)]

[1] German Aerospace Center (DLR), Pfaffenwaldring 38-40, 70569 Stuttgart
[2] German Aerospace Center (DLR), Wankelstr. 5, 70563 Stuttgart

[a)] Corresponding author: reiner.buck@dlr.de
[b)] stefano.giuliano@dlr.de

Abstract. New heat transfer and storage media offer for solar tower systems a much broader temperature range. Higher temperatures allow the integration of steam power cycles with increased efficiency. The present study evaluates modular solar tower plants using solid particles as heat transfer medium (HTM), allowing temperatures up to 1000°C. In a parameter study the influence of upper and lower HTM temperature on levelized cost of electricity (LCOE) is evaluated. The results show a significant impact of the HTM temperature selection, mainly governed by the HTM temperature difference. A high temperature difference results in reduced LCOE. The most important factors for this reduction are the cost decrease of particle inventory, storage containment, and particle steam generator. This decrease is partially offset by an increase in heliostat field and tower cost. The results indicate that the use of solid particles for high efficiency steam power cycles offers unique advantages due to the wide temperature range of the particles.

INTRODUCTION

One of the key performance indicators for the reduction of LCOE of solar power systems is the increase of the temperature level of the solar system and the associated power cycle. Higher working temperatures result in improved efficiency of the power cycle, leading to lower thermal power demand and smaller concentrator fields.

State-of-the-art commercial solar tower systems with storage operate at live steam temperatures up to 540°C. This is limited by the "solar salt", a mixture of 60% $NaNO_3$ and 40% KNO_3, that is currently used as heat transfer medium (HTM) and storage medium. This HTM is used up to salt temperatures of 565°C, at higher temperatures decomposition and corrosion effects become critical. For higher temperatures a new HTM is required. This new HTM should also be cheap enough to provide cost-effective storage capabilities.

In the US study on the next generation of CSP plants ("Concentrating Solar Power Gen3 Demonstration Roadmap") [1] sCO_2 cycles are foreseen for solar power generation, operating at upper temperatures as high as 715°C. Three potential HTM candidates are identified: new molten salt mixtures, solid particles and pressurized gases. For the last option, solid particles are also favored as storage material. The same options exist when advanced steam turbine systems are foreseen for the power block, with live steam temperatures of 600°C or even 620°C.

All three HTM candidates offer flexibility in the selection of the lower and upper temperature levels, which influence the layout of the solar power plant. The selection of these temperatures influences mainly the following aspects: heat exchanger area of the power cycle, receiver efficiency, HTM mass flow, storage mass and volume, and thermal insulation. Some of these parameters have a significant impact on investment cost.

For the analysis, solid particles are selected as HTM. The reason for this selection is the extremely wide acceptable temperature range, up to 1000°C, without a limitation at lower temperatures (e. g. no freezing issues). The low cost of the particles enables also direct use as storage material.

In a previous study [3] the impact of the selection of the upper and lower solid particle operation temperature on the LCOE of a solar tower system with sCO_2 power cycle was investigated. A high efficiency sCO_2 power cycle is characterized by two aspects:

- high upper temperature of the cycle working fluid sCO_2, typically above 600°C
- low temperature spread of the cycle working fluid sCO_2, typically in the range of 150K

The results of this study indicate that the use of solid particles for solar high efficiency sCO_2 power cycles offers unique advantages due to the wide temperature range of the particles.

The objective of this paper is the evaluation of cost trends when a high efficiency steam turbine is used as power cycle. The analysis is based on several simplified assumptions, as some of the components are not fully developed yet and therefore detailed cost and performance data are not available. The results should be understood as trend indicators, not as absolute numbers.

MODEL AND ASSUMPTIONS

For the analysis, a solar tower system with a power rating of 125 MW_e is considered, with a storage size of 12h. The solar tower plant is built as a multi-tower system and consists of 14 solar tower modules delivering heat to a single central power station. Each solar tower module consists of a heliostat field, a tower with a receiver on top, a hot and cold storage containment and the solid particle transport system. The components of the plant are described in the following sections.

Power Cycle

An advanced subcritical steam power cycle with reheat and multiple preheating stages is assumed, as described in [4]. In the steam generator high pressure steam is heated from 261°C to 620°C, in the reheat section the intermediate pressure steam is heated to 620°C. This results in a net cycle efficiency of 43%. With this efficiency, a thermal input power of 291MW_{th} is required from the solar subsystem. For the layout and costing the steam generator is considered as a single heat exchanger.

For the present analysis, the steam generator is treated as a separate cost item, as its cost is strongly influenced by the selected temperature range. For the cost of the remainder of the steam power block, a fixed specific cost of $C_{sp,pc}$ = 700 €/kW_e is assumed. This results in a power cycle cost C_{pc} of 87.5 Mio € (excluding steam generator).

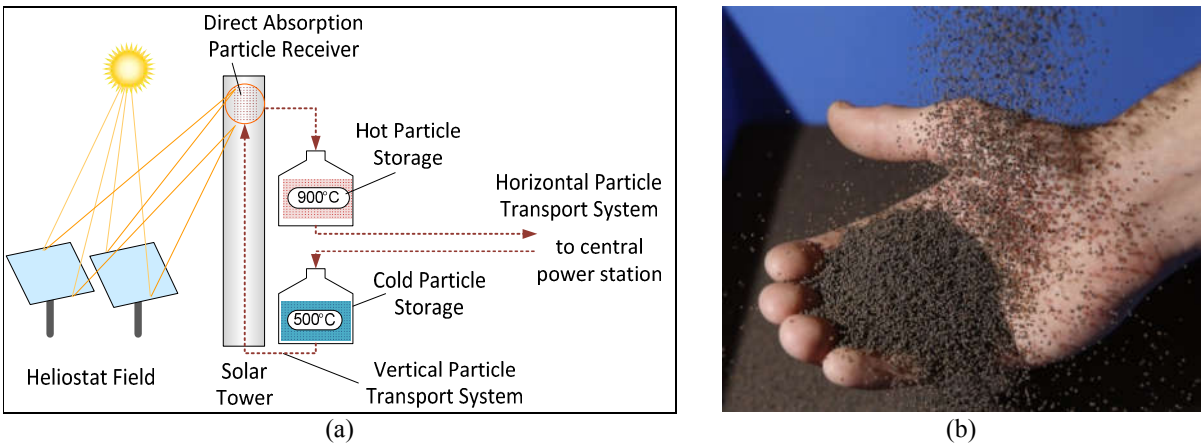

FIGURE 1. Scheme of particle solar tower module (a), solid bauxite particles used as HTM (b)

Solar Tower Module Description

Each of the 14 solar tower modules consists of a receiver with a design point (DP) power of 50MW_{th} , a tower, a heliostat field and a thermal storage. A scheme of a module is shown in Figure 1a. The total thermal system power is 700MW_{th} at DP conditions. With the power cycle demand of 291MW_{th} this represents a solar multiple of 2.4. For the analysis, a site in Northern Chile with an annual direct normal insolation (DNI) of 3583kWh/m²a is assumed. This is an extremely good solar site, however the trend results should be representative for other sites as well.

Heat Transfer and Storage Medium

Bauxite particles are assumed as heat transfer and storage medium, since these particles are relatively inexpensive and allow flexible selection of temperature ranges up to 1000°C. Above this temperature, sintering effects might create problems in particle handling. Also, a lower temperature limit does not exist, and therefore electrical heat tracing (as for molten salts) is not necessary to avoid HTM freezing. A heat capacity of $c_{p,par}$ = 1200 J/kgK and a particle bulk density of ρ_{part} = 2000 kg/m³ are used. Such bauxite particles are produced in huge quantities, e. g. for use in fracking or casting processes. A specific particle cost of $C_{sp,part}$ = 1€/kg is assumed.

Thermal Storage System

For the solar tower system, a thermal storage time of 12h full load operation was assumed, resulting in a total thermal storage capacity E_{st} of 3.49 GWh. This storage capacity is evenly distributed over all solar tower modules. The hot and cold storage containments are either installed inside the tower (eventually using the tower walls as containment walls, with inner insulation) or close to the tower.

Thermal losses through the thermal insulation are neglected. Such losses are usually relatively small. This simplification is also justified since the cost of the insulation is assumed temperature-dependent, i. e. for higher temperatures an improved quality insulation is foreseen. The particle inventory per module is calculated as

$$m_{st} = \frac{E_{st}}{n_{mod} \cdot c_{p,part} \cdot (T_{r,ex} - T_{r,in})} \quad (1)$$

Another 10% of this particle mass is added to obtain the total particle mass, to account for particles in other components, e. g. the transport containments. The cost of the particle inventory C_{part} is then calculated as

$$C_{part} = 1.1 \cdot m_{st} \cdot C_{sp,part} \quad (2)$$

The cost of the storage containment C_{stc} is calculated from the surface area A_{stc} of the containment. A cylindrical containment with the cylinder height being twice the cylinder diameter is assumed. From the particle inventory, the volume of a fully charged containment is calculated, and then the cylinder diameter and the surface area are derived. A temperature-dependent area-specific insulated structure cost $C_{A,sp,is}$ [€/m²] is calculated as follows:

$$C_{A,sp,is}(T_{st}) = 1000 \cdot \left(1 + f_{ins} \cdot \frac{(T_{st} - 600)}{400}\right) \quad (3)$$

The factor f_{ins} describes the cost share of the thermal insulation. In the above formulation, the insulation cost part is doubled when the storage temperature T_{st} (in °C) is increased from 600°C to 1000°C. A value of f_{ins} = 0.3 is assumed for the insulation cost share. The storage containment cost is the sum of the cost of the hot and cold storage containments:

$$C_{stc} = A_{stc} \cdot C_{A,sp,is}(T_{r,ex}) + A_{stc} \cdot C_{A,sp,is}(T_{r,in}) \quad (4)$$

The total cost of the storage system C_{st} is then obtained as the sum of C_{part} and C_{stc}.

Solar Receiver

The receiver technology is based on the centrifugal particle receiver technology CentRec® [5]. This receiver technology is currently under development at DLR. The receiver is based on the direct absorption principle, meaning that the dark bauxite particles are irradiated directly by the concentrated solar power and get heated from the absorbed radiation. A first demonstration receiver with about 2.5MW$_{th}$ peak power was installed at the DLR solar tower test facility in Jülich, Germany. Due to constraints of the test platform in the solar tower test facility, which is located about midway up the tower, a thermal power output of up to 500kW$_{th}$ is expected. Nearly 70h of solar testing were carried out, and receiver outlet temperatures up to 965°C (average) were achieved [6].

The receiver has a circular aperture facing south (the plant is on the southern hemisphere). The aperture area A_{ap} and the tilt angle vary according to the selected temperature range and are determined during the solar system

optimization. A simplified receiver model is considered, with the absorbed power $P_{r,abs}$ defined as a function of intercepted power $P_{r,int}$ and receiver exit temperature $T_{r,ex}$ by

$$P_{r,abs} = \alpha \cdot P_{r,int} - \varepsilon\sigma\, A_{ap}\, T_{r,ex}^4 - h\, A_{ap}\, (T_{r,ex} - T_{amb}) \tag{5}$$

with effective solar absorptivity α = 0.95, effective thermal emissivity ε = 0.9 and a convective heat loss coefficient of h = 30 W/m²K. Note that in this correlation all temperatures must be used in [K]. For the ambient temperature T_{amb} a value of 300K is taken.

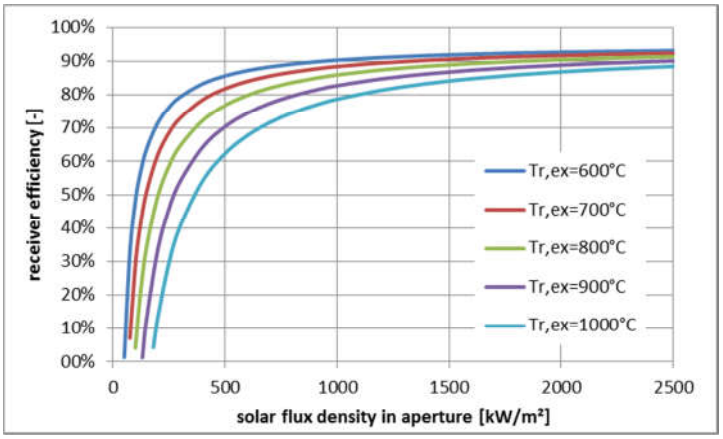

FIGURE 2. Receiver efficiency as a function of average flux density in aperture

The receiver cost is described by two contributing factors: one depending only on the receiver aperture area A_{ap}, another one depending on the surface area of the internal insulated structure and the receiver exit temperature. The surface area of the internal insulated structure is calculated for a cylindrical receiver chamber with a diameter of 1.3 times the aperture diameter and a depth of two times the aperture diameter. The area of the insulated structure $A_{r,is}$ is then composed of area of the cylinder wall and the area of the flat back wall of the cylinder. The total cost of the receiver system C_r is calculated as

$$C_r = 70000 \cdot A_{ap} + A_{r,is} \cdot C_{A,sp,is}(T_{r,ex}) \tag{6}$$

Heliostat Field and Tower

The heliostat field consists of a large number of rectangular heliostats, tracked in two axes. For each heliostat, a dimension of 12.84m width and 9.45m height is assumed, with a net reflective area of 121m². A reflectivity of 88% is assumed, accounting for the mirror reflectivity and an average dirt coverage of the mirrors. A specific cost $C_{sp,f}$ of 100 €/m² installed heliostat field is assumed.

For each temperature range, the heliostat field layout and the number of heliostats are optimized using the simulation tool HFLCAL [7]. A radially staggered field layout is selected. As a result, the total heliostat field area A_f is obtained. The total cost of the heliostat field C_{field} is calculated as

$$C_{field} = A_f \cdot C_{sp,f} \tag{7}$$

A tower is required to locate the solar receiver at a suitable height above the heliostat field. The tower height is dominated by the heliostat field and receiver configuration, and is optimized together with other parameters.

The cost of the tower is assumed as [8]

$$C_t = 1767767 \cdot e^{6.931E-3 \cdot H_t} \tag{8}$$

Steam Generator

A moving bed particle heat exchanger (Fig. 3) is foreseen for the steam generator / reheater of the power cycle. In this heat exchanger type, the solid particles are moving slowly across the heat exchanger tubes, driven by gravity [9]. The mass flow is controlled by variable gate valves at the cold exit of the heat exchanger. The required heat transfer area of this heat exchanger is calculated as

$$A_{HX} = \frac{P_{el}/\eta_{pc}}{h_{SG} \cdot \Delta T_{log}} \tag{9}$$

In [9] convective heat transfer coefficients up to 240 W/m²K were measured for a tube bundle type heat exchanger with particle inlet temperatures ranging from 355°C to 470°C. Since the particle heat exchanger for a steam power cycle is operated at significantly higher temperatures, radiative heat transfer will improve heat transfer. Therefore, a constant heat transfer coefficient h_{SG} of 300 W/m²K is assumed. The logarithmic temperature difference ΔT_{log} for a heat exchanger in cross-flow configuration is calculated based on the solid particle temperature selection and the power cycle temperature levels. The steam generator temperatures are 620°C for the steam outlet and 261°C for the preheated water inlet.

The steam generator material temperatures are mainly defined by the steam conditions, as the highest heat transfer resistance will be between particles and tube material, i. e. the tube material temperatures will be quite independent of particle temperatures. Thus, the heat exchanger cost is only a function of the heat transfer area.

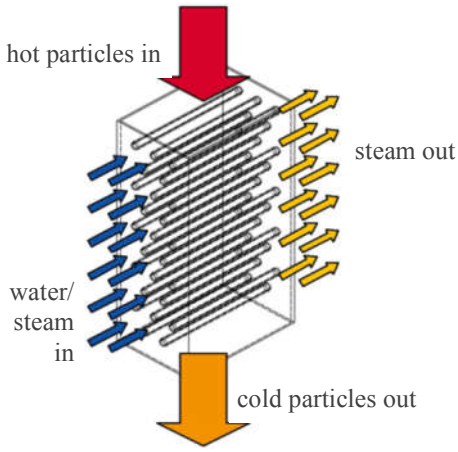

FIGURE 3. Scheme of moving bed particle steam generator

For the cost of the steam generator a correlation was derived using the MATCHE data base [10] assuming Inconel 625 as tube material. With a correction factor the high pressure of the steam system, a translation from 2014 cost into actual cost and after converting from $ to € this resulted in the following correlation:

$$C_{HX} = = \ 128122 \cdot A_{HX}^{0.66} \tag{10}$$

Particle Transport System

The multi-tower system needs particle transportation in two ways: lifting the “cold” particles up to the receiver inlet (“vertical” particle transport) and transporting the particles between a solar tower module and the central power station (“horizontal” particle transport). After being cooled down in the steam generator of the central power block, the cold particles are transported back to the solar tower modules and are either lifted up to the receiver (when enough solar power is available) or lifted to the inlet of the cold storage container. When more solar power is available than the power cycle takes, particles from the cold storage are lifted up to the receiver and, after being heated up, put into the hot storage. Particle transport downwards is always accomplished by gravitational flow.

Vertical particle transport

A mine hoist system is foreseen for the vertical particle transport. Repole et al. [11] have made a conceptual design for a hoist for a solar demonstration system with a thermal capacity of 60MW_{th}. Since the selected solar tower module size is close to this capacity, this mine hoist design was taken as base value for the calculation of the cost for the specific configuration. Scaling factors are applied for conditions differing from the original design values. The used correlation is (after currency conversion from $ to €):

$$C_{tr} = 425000 \cdot \left\{1 + k_T \left(\frac{T_l - T_{l,0}}{T_{l,0}}\right)\right\} \cdot \left\{1 + k_m \left(\frac{\dot{m} - \dot{m}_0}{\dot{m}_0}\right)\right\} \cdot \left\{1 + k_H \left(\frac{H_l - H_{l,0}}{H_{l,0}}\right)\right\} \quad (11)$$

The scaling factors are selected as $k_T = 0.1$, $k_m = 0.5$ and $k_H = 0.2$.

Horizontal particle transport

For transportation between the solar tower modules and the central power station a number of trucks are foreseen, each transporting insulated containers (one for hot and another for cold particles). One truck is serving one module. This is sufficient for the highest particle mass flows (i. e. the smallest temperature particle difference of 200K), for lower mass flows this is oversized and might be reduced even further. The trucks are continuously operated whenever the power cycle is producing electricity, e. g. also during night time. As the paths between the solar tower modules and the central power block are clearly defined, fully autonomous trucks are foreseen. The cost of each truck system is estimated as $C_{tr,h}$ = 280000€ and includes the truck and 6 insulated containers (3 for cold particles and 3 for hot particles). This enables continuous operation of the horizontal particle transport system, with one container discharged, one container being transported, and one container being charged at the same time.

Other Performance Assumptions

Thermal losses through the insulation are neglected, as they are usually very small. The parasitic power consumption of some components (rotation drive of receiver, horizontal particle transport system, power cycle parasitics) was also excluded from the analysis. Vertical particle transport power was accounted for.

OPTIMIZATION OF SYSTEM CONFIGURATION

A number of system configurations are evaluated, with the levelized cost of electricity (*LCOE*) as the evaluation criteria. The total capital expenditures *CAPEX* is the sum of all module cost plus the cost of the central power block (steam generator and power cycle). Contingencies of 30% are added to the total *CAPEX*. Annual operational expenditures *OPEX* are assumed as 2% of the total *CAPEX*. The annual electric power production is obtained from the HFLCAL layout optimization, based on the annual thermal energy. The evaluation of the *LCOE* is calculated using a simplified annuity approach as follows:

$$LCoE = \frac{CAPEX \cdot f_{annuity} + OPEX}{E_{el,annual}} \quad (12)$$

The annuity factor $f_{annuity}$ is based on interest rate and the depreciation period [9]. With an interest rate of 7% and a depreciation period of 25a an annuity factor of 8.58% is obtained.

Each configuration is defined by a specific receiver inlet and outlet temperature. For each temperature set, the solar subsystem is optimized for minimal *LCOE*. The following parameters are varied during the optimization: receiver aperture area, receiver tilt angle, tower height and field layout. A radially staggered field layout is assumed. The simulation tool HFLCAL [7] was used to determine the optimal parameters for each temperature set.

RESULTS

The parameter study was carried out using receiver inlet temperatures of 400°C and 500°C. Temperature differences between receiver exit and inlet temperature were between 200°C and 600°C, with an upper limit for the

receiver exit temperature of 1000°C. Figure 4a shows the resulting *LCOE* for the selected parameter sets. It is obvious that the higher the receiver exit temperature the lower the *LCOE* is. For a given receiver exit temperature, lower receiver inlet temperatures result in lower *LCOE*. The *LCOE* of the worst case (500°C/700°C) is more than 14% higher than in the best case (400°C/1000°C).

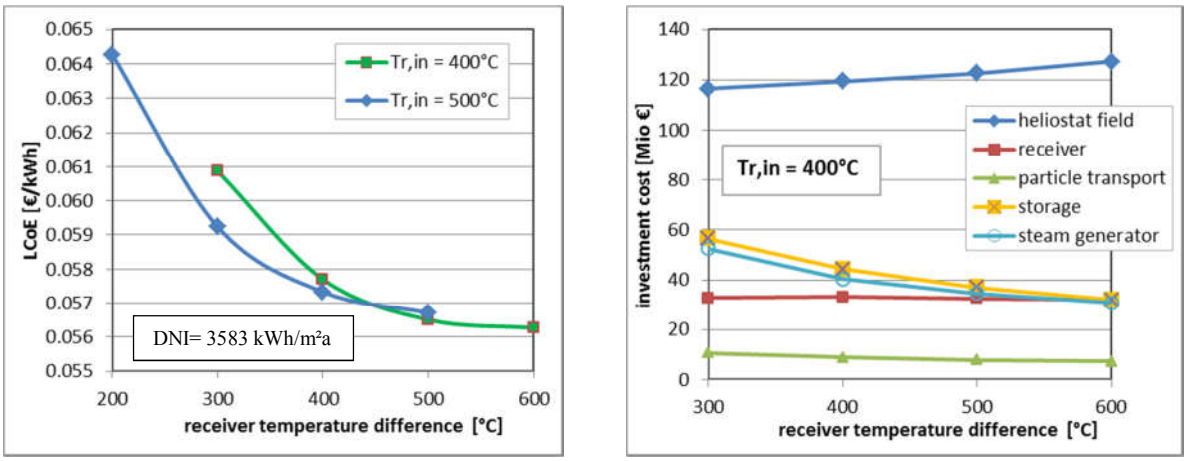

(a) (b)

FIGURE 4. Levelized cost of electricity for the site in Chile (a) and component cost (b) vs. HTM temperature difference

Figure 4b shows the cost contributions of the most important factors for the *LCOE* change. The shown characteristic is mainly resulting from a significant cost decrease in the storage cost and in the steam generator cost, when the temperature difference is increased. A minor cost decrease occurs in the particle transport system, mainly due to reduced mass flow requirements. On the other hand, the cost of heliostat field and tower increase with increasing receiver exit temperature. This is caused by decreasing receiver efficiency, requiring more heliostats and a higher tower to deliver the required thermal power. Interesting to see is that the predicted cost of the storage system is as low as 9.2 €/kWh, less than half of the cost of a molten salt storage system.

CONCLUSIONS

Solid particle systems offer a high flexibility in the selection of temperature levels. The increased temperature allows the integration of advanced high efficiency steam power cycles. In addition the temperature spread between upper and lower particle temperature can be optimized in a wide range. The present study evaluates modular solar tower plants using solid particles as HTM, allowing HTM temperatures up to 1000°C. In a parameter study the influence of the lower and upper HTM temperature on *LCOE* is evaluated.

The results show a significant impact of the HTM temperature selection, mainly governed by the HTM temperature difference. A high temperature difference results in reduced *LCOE*. The most important factors for this reduction are the reductions in particle inventory, storage containment, and particle steam generator. This reduction is partially offset by an increase in heliostat field and tower cost.

The results indicate that the use of solid particles for solar high efficiency steam power cycles offers significant advantages due to the wide temperature range of the particles. In addition, the modular solar tower design will allow simple adaptation to other power levels and capacity factors.

It should be stated that several of the used cost correlations are “best guesses”, as currently no sound database exists for many of the new components. These correlations should be refined by future work to improve the quality of the results.

NOMENCLATURE

Symbols	Unit	Description
A	$[m^2]$	area
C	[€]	cost
c_p	[J/kgK]	heat capacity
E	[J]	energy
H	[m]	tower height
h_{SG}	$[W/m^2K]$	convective heat transfer coeff.
m	[kg]	mass
n_{mod}	[-]	number of solar tower modules
$LCOE$	[€/kWh]	levelized cost of electricity
P	[W]	power
T	[°C]; [K]	temperature
ρ	$[kg/m^3]$	density
η	[-]	efficiency
σ	$[W/m^2K^4]$	Stefan–Boltzmann constant

Abbreviations

CAPEX: capital expenditures
CSP: concentrating solar power
DNI: direct normal insolation
DP: design point
HTM: heat transfer medium
OPEX: operational expenditures

Subscripts	
abs	absorbed
annual	annual value
ap	aperture
el	electric
ex	exit
f	field
h	horizontal
SG	steam generator
in	inlet
int	intercepted
is	insulation structure
mod	(solar tower) module
part	particle
pc	power cycle
r	receiver
st	storage
stc	storage containment
sp	specific
th	thermal
tr	transport
t	tower
v	vertical

REFERENCES

1. Concentrating Solar Power Gen3 Demonstration Roadmap; Technical Report NREL/TP-5500-67464, January 2017. Available at: www.nrel.gov/publications.
2. S. Giuliano et al., HPMS - High Performance Molten Salt Tower Receiver System. Project Report, DLR Stuttgart (2017). https://doi.org/10.2314/GBV:1010747207
3. R. Buck, S. Giuliano: Impact of Solar Tower Design Parameters on sCO_2-based Solar Tower Plants, Proc. 2nd European Supercritical CO_2 Conference, August 30-31, 2018, Essen, Germany (to be published)
4. M. Puppe et al. (2017). Techno-Economic Optimization of Molten Salt Solar Tower Plants. Pres. at SolarPACES 2017, Chile.
5. M. Ebert, L. Amsbeck, A. Jensch, J. Hertel, J. Rheinländer, D. Trebing, R. Uhlig, R. Buck (2016). Upscaling, Manufacturing and Test of a Centrifugal Particle Receiver. PowerEnergy2016-59252, Proc. ASME Energy Sustainability Conference, 26.-30. June 2016, Charlotte, United States.
6. M. Ebert, L. Amsbeck, J. Rheinländer, B. Schlögl-Knothe, S. Schmitz, M. Sibum, R. Uhlig, R. Buck (2018). Operational Experience of a 500 kW_{th} Centrifugal Particle Receiver System, SolarPACES 2018 (to be published)
7. P. Schwarzbözl, R. Pitz-Paal, M. Schmitz (2009). Visual HFLCAL - A Software Tool for Layout and Optimisation of Heliostat Fields. Proc. SolarPACES 2009, Berlin.
8. G. Weinrebe, F. von Reeken, M. Wöhrbach, T. Plaz, V. Göcke, M. Balz (2014). Towards Holistic Power Tower System Optimization. Energy Procedia, ISSN: 1876-6102, Vol: 49, Page: 1573-1581
9. T. Baumann and S. Zunft (2014). Experimental Investigation on a Moving Bed Heat Exchanger used for discharge of a particle-based TES for CSP. Eurotherm Seminar #99 - Advances in Thermal Energy Storage, 28.05.-30.05.2014, Lleida, Spain. ISBN 978 84 697 0467 7
10. http://matche.com/equipcost/Exchanger.html (last visited 22.06.2018)
11. K. D. Repole and S. M. Jeter (2016). Design and Analysis of a High Temperature Particulate Hoist for Proposed Particle Heating Concentrator Solar Power Systems. ASME Energy Sustainability 2016. doi:10.1115/ES2016-59619.
12. A. Roy, W. Meinecke, M. Blanco (1997). "Introductory Guidelines for Preparing Reports on Solar Thermal Power Systems", SolarPACES Rep. No. III-3/97.